Mechanical and Microstructural Properties of Pediatric Anterior Cruciate Ligaments and Autograft Tendons Used for Reconstruction

Elaine C. Schmidt,* MS, Matthew Chin,* BS, Julien T. Aoyama,† BA, Theodore J. Ganley,† MD, Kevin G. Shea,‡ MD, and Michael W. Hast,*§ PhD

Investigation performed at the Biedermann Laboratory for Orthopaedic Research, Department of Orthopaedic Surgery, University of Pennsylvania, Philadelphia, Pennsylvania, USA

Background: Over the past several decades, there has been a steady increase in pediatric anterior cruciate ligament (ACL) tears, particularly in young female basketball and soccer players. Because allograft tissue for pediatric ACL reconstruction (ACLR) has shown high rates of failure, autograft tissue may be the best option for ACLR in this population. However, differences in the structure and mechanical behavior of these tissues are not clear.

Purpose: To characterize the mechanical and microstructural properties in pediatric ACLs and autograft tissues using a rare cadaveric cohort (mean age, 9.2 years).

Study Design: Descriptive laboratory study.

Methods: ACLs, patellar tendons, quadriceps tendons, semitendinosus tendons, and iliotibial bands (ITBs) were harvested from 5 fresh-frozen pediatric knee specimens (3 male, 2 female) and subjected to a tensile loading protocol. A subset of contralateral tissues was analyzed using bright-field, polarized light, and transmission electron microscopy.

Results: Patellar tendons exhibited values for ultimate stress (5.2 ± 3.1 MPa), ultimate strain (35.3% ± 12.5%), and the Young modulus (27.0 ± 8.8 MPa) that were most similar to the ACLs (5.2 ± 2.2 MPa, 31.4% ± 9.9%, and 23.6 ± 15.5 MPa, respectively). Semitendinosus tendons and ITBs were stronger but less compliant than the quadriceps or patellar tendons. ITBs exhibited crimp wavelengths (27.0 ± 2.9 μm) and collagen fibril diameters (67.5 ± 19.5 nm) that were most similar to the ACLs (24.4 ± 3.2 μm and 65.3 ± 19.9 nm, respectively).

Conclusion: The mechanical properties of the patellar tendon were almost identical to those of the ACL. The ITB exhibited increased strength and a similar microstructure to the native ACL. These findings are not entirely congruent with studies examining adult tissues.

Clinical Relevance: These results can be used to inform further clinical research. In particular, they justify a further examination of the biomechanical and microstructural properties of the ITB in the context of its role as an autograft tissue in pediatric ACL reconstruction.

Keywords: pediatric; ACL reconstruction; mechanical properties; microstructural properties; patellar tendon grafts; quadriceps tendon grafts; hamstring grafts

A large amount of research has been devoted to characterizing the mechanical and microstructural properties of the tendons and ligaments surrounding the adult human knee. Because of the extreme rarity of pediatric cadaveric specimens, relatively little is known about these properties in the pediatric population. While the effects of senescent aging on the tensile properties of these structures have been established,[23,35,58] extrapolating these data to prepubescent ages is inadequate. Over the past several decades, the clinical need for these data in pediatric orthopaedics has grown in parallel with the steady increase of diagnosed ligament tears in skeletally immature patients.[3,11,27,36] This trend has been attributed to several factors, including increased participation in youth sports, sport specialization, year-round play, and increase in the number of adolescents competing at higher levels of competition.[13]

The Orthopaedic Journal of Sports Medicine, 7(1), 2325967118821667
DOI: 10.1177/2325967118821667

Pediatric anterior cruciate ligament (ACL) tears account for the majority of these knee injuries, seen particularly in young female soccer and basketball athletes.[17,46]

In the pediatric patient, the surgical treatment of ACL deficiency is complicated by the potential risk of injuries to the physis. There is currently a large debate and practice variation in the initial management, operative timing, and operative technique for pediatric ACL reconstruction (ACLR). Adolescents approaching skeletal maturity can be managed similarly to adults with complete transphyseal reconstruction.[15] However, if the patient's physes are still open, physeal-sparing or partial transphyseal techniques are often preferred to prevent premature physeal closure and postoperative growth disturbance.[15,28] In choosing the best course of treatment, the surgeon must consider both the pediatric patient's bone growth potential and the need for graft stability and durability in the face of return to sport and a longer remaining life span.[41]

Graft choices for ACLR include the hamstring tendon, bone–patellar tendon–bone, quadriceps tendon, and iliotibial band (ITB). Autografts are generally preferred; allografts have been shown to have increased failure rates in younger and more active children because of slower incorporation and a higher infection rate.[14] Each of these graft options has been shown to be clinically successful but also possesses its own suite of risks. Unresolved issues regarding harvesting, biological incorporation, and donor site morbidity remain controversial.[9,25,54,57] ITB grafts may benefit pediatric patients because of the physeal-sparing benefits of the procedure,[15] but bone–patellar tendon–bone and hamstring grafts for reconstruction are more widely used.[9,14]

There remains a dearth of knowledge about the mechanical and structural properties of autograft tissues in the pediatric population. It is currently unknown whether the patellar tendon, ITB, or hamstring tendon possesses the appropriate structural properties and mechanical durability to be well suited to act as an ACL surrogate. Gaining a better understanding of these relationships will likely improve surgical outcomes in pediatric patients, particularly as the frequency of ACLR continues to accelerate.[40] While many in vitro studies have examined the material properties of ACLs and common grafts used for knee ligament reconstruction in adults[47,48] and in skeletally immature animal models,[7,10,59] to our knowledge, no analogous studies have been conducted in the pediatric population. Therefore, the purpose of this study was to characterize the mechanical properties and microstructure of ACLs and the most common tendons used for pediatric ACLR.

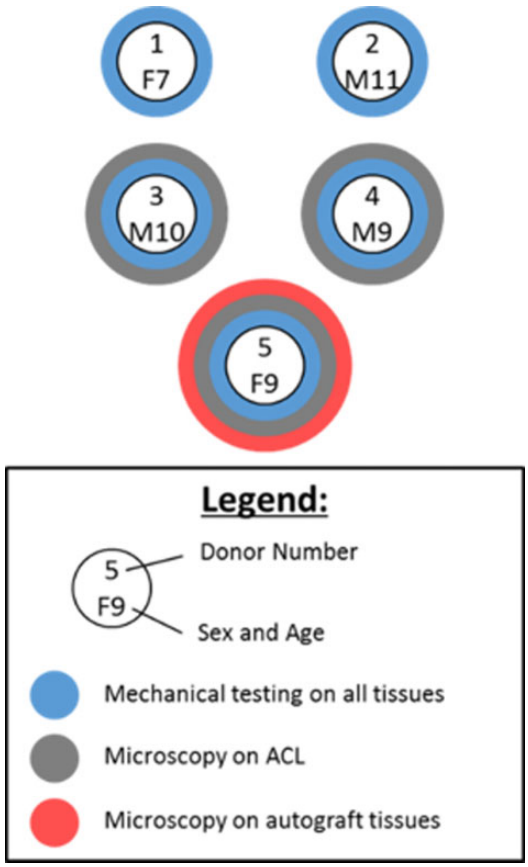

Figure 1. Schematic showing testing designations for the procured pediatric knee specimens. ACL, anterior cruciate ligament. F, female; M, male.

METHODS

Five fresh-frozen pediatric cadaveric specimens (3 male, 2 female; mean age, 9.2 years) were acquired through a donation from AlloSource. Because of the rarity of this cohort, portions of the knees were dissected, refrozen at –20°C, and sent to various research laboratories throughout the country. This study received complete ACLs,

§Address correspondence to Michael W. Hast, PhD, Biedermann Laboratory for Orthopaedic Research, Department of Orthopaedic Surgery, University of Pennsylvania, 3737 Market Street, Suite 1050, Philadelphia, PA 19104, USA (email: hast@pennmedicine.upenn.edu).
*Biedermann Laboratory for Orthopaedic Research, Department of Orthopaedic Surgery, University of Pennsylvania, Philadelphia, Pennsylvania, USA.
†Children's Hospital of Philadelphia, Philadelphia, Pennsylvania, USA.
‡Department of Orthopaedic Surgery, Stanford University, Stanford, California, USA.
One or more of the authors has declared the following potential conflict of interest or source of funding: This study was supported by the Penn Center for Musculoskeletal Disorders Histology Core (NIH P30-AR06919) and the Electron Microscopy Resource Laboratory of the University of Pennsylvania, and pediatric tissues were donated by AlloSource. T.J.G. receives research support from AlloSource, Vericel, and Liberty Surgical and has received hospitality payments from Arthrex. K.G.S. receives research support from AlloSource, Vericel, DePuy Synthes, and Sanofi-Aventis and is an unpaid consultant for Clinical Data Solutions. M.W.H. receives research support from DePuy Synthes, Integra LifeSciences, and Zimmer Biomet. AOSSM checks author disclosures against the Open Payments Database (OPD). AOSSM has not conducted an independent investigation on the OPD and disclaims any liability or responsibility relating thereto.
Ethical approval was not sought for the present study.

patellar tendons, quadriceps tendons, semitendinosus tendons, and ITBs from a single limb for all 5 donors, primarily for the purposes of mechanical testing (Figure 1). In some cases, tissues from the contralateral limb were also available for testing, and microstructural analyses were performed on these specimens. Specifically, the contralateral ACLs from donor 3 (male, aged 10 years) and donor 4 (male, aged 9 years) were available for hematoxylin and eosin (H&E) histology, polarized light microscopy, and transmission electron microscopy (TEM) analysis. All of the contralateral tendons and ligaments from donor 5 (female, aged 9 years) were also available and were used for these microstructural analyses. This allowed for a comparison between the ACL and different candidate autograft tissues within a single specimen.

Mechanical Testing

Mechanical testing was performed on a total of 24 specimens from the 5 donors. One ACL (donor 1) was excluded from testing because of its small size and poor quality, which made it impossible to examine. All specimens were tested as single-ply and were not folded into multibundle constructs. The ACLs were dissected and tested as 1 unit containing both the anteromedial and posterolateral bundles. Tendons were prepared for testing by cutting them into standard dog-bone shapes at the midsubstance (ACL, patellar tendon, quadriceps tendon) (Figure 2A) or distal substance (semitendinosus tendon and ITB) with a custom-built jig. Cross-sectional areas (CSAs) were measured along the gauge length of prepared specimens with a noncontact laser-based measurement system and were averaged (Figure 2B). Specimen ends were then placed in custom aluminum clamps and attached to a 3-kN load cell on a universal testing frame (ElectroForce 3330; TA Instruments) to perform uniaxial tensile testing (Figure 2, C and D). Tissues were kept hydrated throughout sample preparation and mechanical testing.

The tensile loading protocol was based on a previously published study.[33] Briefly, the tissue was preloaded from a slack position to 5 N and then preconditioned with 10 cycles between 10 and 5 N at a 0.4% strain rate. After dwelling at 5 N, the specimen underwent a stress-relaxation protocol, followed by ramp to failure at a constant quasistatic strain rate of 0.03% per second (Appendix Figure A1). Failure of the specimens was confirmed mechanically by a sharp decrease in force and visually by the observance of frayed fibers at the midsubstance. Global longitudinal strain was measured using the known gauge length of the dog-boned specimen and the change in displacement of the actuator on the universal testing frame. The viscoelastic parameter of stress relaxation was calculated as the percentage change in stress from peak stress to equilibrium). A bilinear constitutive model with least squares fit[8,29,55] (Appendix Figure 2A) was applied to the stress-strain data to quantify the moduli in the toe and linear regions as well as the stress and strain values corresponding to the following transition point:

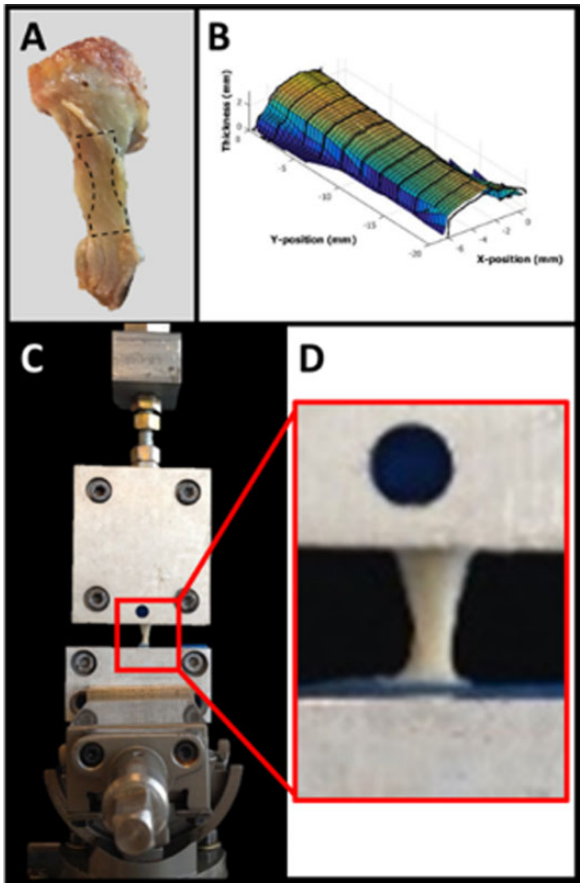

Figure 2. (A) Representative image of a harvested pediatric bone–patellar tendon–bone segment. The dashed lines show the location where the specimens were cut into dog-bone shapes at the midsubstance. (B) Topographical map of the middle portion of a dog-boned specimen taken with a laser-based 3-dimensional scanner. (C, D) Photograph of the tensile testing setup showing how the custom-made grips and specimens were subjected to tensile loads.

$$\sigma = \begin{cases} E\varepsilon & \varepsilon \le \varepsilon^* \\ E'(\varepsilon - \varepsilon^*) + E\varepsilon^* & \varepsilon > \varepsilon^* \end{cases},$$

where E is the slope of the toe modulus, E' is the slope of the Young modulus, ε is the strain, ε^* is the transition strain, and σ is the stress. Although the toe region is nonlinear, the model produced a practical and conservative approximation of the toe modulus and transition point. Stiffness was calculated as the slope of the load-displacement curve, and strain energy density, which represents the energy absorbed before failure, was calculated as the area under the stress-strain curve.

Histology and Polarized Light Microscopy

Samples for histology were fixed in 10% neutral buffered formalin and embedded in paraffin. Serial sections ($\sim$8 μm) were stained with H&E and viewed with bright-field

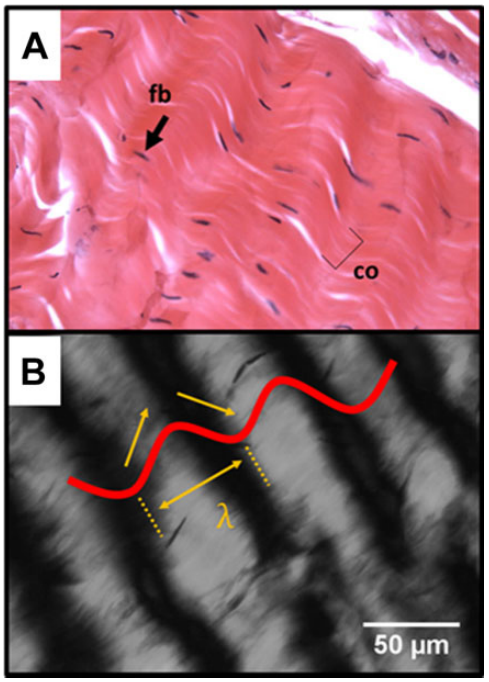

Figure 3. (A) Hematoxylin and eosin–stained pediatric patellar tendon specimen viewed using bright-field microscopy. Fibroblast nuclei (fb) and collagen (co) are indicated. (B) Under polarized light microscopy, discrete crimps are identified, and the wavelength (λ) is measured in micrometers. 20× magnification.

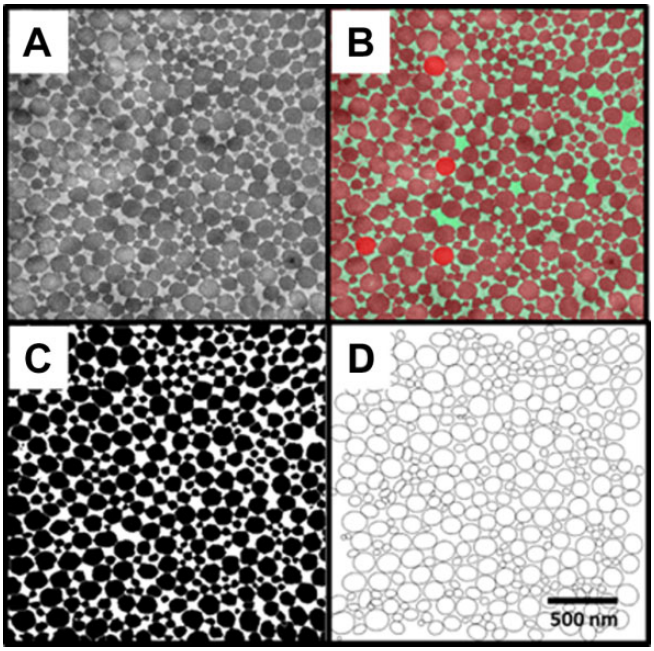

Figure 4. Transmission electron microscopy analysis protocol. (A) Micrograph for a pediatric patellar tendon specimen. (B) Machine learning segmentation of fibrils (red) from the background (green). (C) Complete segregation of the fibrils using thresholding and watershed techniques. (D) Ellipse fit to each individual fiber.

microscopy (Figure 3A). Ten randomly chosen regions (0.35 × 0.26 mm^2 each) were evaluated for each specimen, and the mean cell density was measured using ImageJ software (National Institutes of Health). Collagen crimp properties were examined using polarized light microscopy, as previously described in the literature.[30] Crimp wavelength was determined by crossing the polarizer and analyzer at 90°, rotating the specimens until maximal extinction in the dark crimp bands occurred, and calculating the distance spanned by a dark and light band unit (Figure 3B).[12,60]

Scaled images from 10 randomly chosen regions (0.35 × 0.26 mm^2 each) were obtained, and consecutive crimp wavelengths were individually measured and averaged. A minimum of 100 crimps were analyzed over the 10 images for each specimen. The quality of the histology sections for 1 ACL (donor 4) was determined to be too poor to be included in subsequent analyses, and it was consequently excluded.

Transmission Electron Microscopy

Tissues for the electron microscopic examination were fixed with 2.5% glutaraldehyde and 2.0% paraformaldehyde in 0.1 M sodium cacodylate buffer overnight at 4°C. After subsequent buffer washes, the samples were post-fixed in 2.0% osmium tetroxide for 1 hour at room temperature and rinsed in DH_2O before en bloc staining with 2% uranyl acetate. After dehydration through a graded ethanol series, the tissue was infiltrated and embedded in EMbed 812 (Electron Microscopy Sciences). Thin sections were stained with uranyl acetate and lead citrate and examined with an electron microscope (1010; JEOL USA) fitted with a digital camera and AMT Advantage image capture software (Advanced Microscopy Techniques).

Ten micrographs were obtained at 60,000× magnification, transverse to the load-bearing axis for each specimen, and each micrograph was analyzed using a semiautomated protocol in ImageJ/Fiji software[44] (Figure 4A). A machine learning classifier was trained to distinguish the darker fibrils from the lighter background of the micrograph (Figure 4B). The fibrils were then completely differentiated from the background using a binary thresholding algorithm and separated from other fibril edges using a watershed segmentation algorithm (Figure 4C). Each discrete fibril was fit with an ellipse, and the Feret minor diameter was determined, which reduced errors introduced by unintended oblique sectioning of the fibrils (Figure 4D). The distributions of fibril diameters were fit using a kernel density estimation to show the modality of their profiles. A minimum of 3000 fibrils were analyzed over the 10 TEM images for each specimen.

Statistical Analyses

Although the sample size was small, statistical differences between the groups were determined by performing 1-way analysis of variance with $\alpha = 0.05$. When tests for both

TABLE 1
Results for Pediatric ACLs and Candidate Graft Tendons[a]

	n	Stress Relaxation, %	Ultimate Stress, MPa	Ultimate Strain, %	Young Modulus, MPa	Stiffness, N/mm	Strain Energy Density, MPa
ACL	4	26.5 ± 9.2	5.2 ± 2.2	31.4 ± 9.9	23.6 ± 15.5	39.6 ± 17.6	0.8 ± 0.4
Patellar	5	40.6 ± 4.8	5.2 ± 3.1	35.3 ± 12.5	27.0 ± 8.8	17.5 ± 5.9	1.2 ± 0.9
Quadriceps	5	33.2 ± 9.8	12.1 ± 8.3	38.9 ± 15.7	61.9 ± 65.0	39.1 ± 31.6	2.5 ± 1.9
Semitendinosus	5	26.7 ± 4.7	29.0 ± 11.6	20.8 ± 7.2	197.2 ± 34.4	100.8 ± 17.6	3.1 ± 1.3
ITB	5	22.6 ± 3.0	29.0 ± 10.6	28.1 ± 10.6	161.7 ± 100.2	61.6 ± 22.5	3.8 ± 1.3
P values							
ACL vs patellar		.02[b]	>.99	.85	.94	.51	.74
ACL vs quadriceps		.39	>.99	.72	.56	>.99	.18
ACL vs semitendinosus		.97	.03[b]	.56	<.01[b]	.14	.10
ACL vs ITB		.64	.03[b]	.67	.01[b]	>.99	.03[b]

[a]Data are shown as mean ± SD unless otherwise indicated. ACL, anterior cruciate ligament; ITB, iliotibial band.
[b]Statistically significant ($P < .05$).

TABLE 2
Toe Region Results for Pediatric ACLs and Candidate Graft Tendons[a]

	n	Transition Stress, MPa	Transition Strain, %	Toe Modulus, MPa
ACL	4	0.8 ± 0.3	5.5 ± 1.9	13.1 ± 7.2
Patellar	5	0.4 ± 0.2	2.4 ± 0.7	16.9 ± 6.0
Quadriceps	5	1.0 ± 1.1	2.8 ± 0.3	33.6 ± 37.7
Semitendinosus	5	3.0 ± 1.6	5.1 ± 2.7	65.2 ± 13.5
ITB	5	2.8 ± 0.9	6.2 ± 5.2	58.9 ± 29.5
P values				
ACL vs patellar		>.99	.04[b]	>.99
ACL vs quadriceps		>.99	.07	>.99
ACL vs semitendinosus		.18	>.99	.02[b]
ACL vs ITB		.18	>.99	.05

[a]Data are shown as mean ± SD unless otherwise indicated. ACL, anterior cruciate ligament; ITB, iliotibial band.
[b]Statistically significant ($P < .05$).

normality (Shapiro-Wilk, $\alpha = 0.05$) and equal variance ($\alpha = 0.05$) passed, the post hoc Holm-Sidak test was used to perform multiple comparisons of the various tendons versus the ACL, which was defined as the control. When tests for normality and equal variance failed, the Kruskal-Wallis test was instead utilized, and the post hoc Dunn test was used to perform multiple comparisons.

RESULTS

Mechanical Testing

The patellar tendon exhibited mechanical properties that were most similar to those of the ACL, particularly for ultimate stress, the Young modulus, and ultimate strain (Table 1 and Appendix Table A1). The toe region properties of the ACL and patellar tendon were also similar, particularly for toe modulus and transition strain (Table 2 and Appendix Table A2). The pediatric semitendinosus tendon was stronger and less compliant than the ACL and other graft candidates as evidenced by its considerably larger values for the Young modulus, stress, and strain energy density. The patellar tendon exhibited the greatest percentage of stress relaxation, while the values for the ACL, quadriceps tendon, semitendinosus tendon, and ITB were relatively similar.

Histology, Polarized Light Microscopy, and TEM

Although the specimens exhibited more similarities than differences from bright-field microscopy analysis, H&E-stained sections did show higher concentrations of fibroblasts in the ACL and ITB samples from donor 5 compared with the other tendons (Figure 5 and Table 3). The mean fibroblast cell count in the ITB was considerably greater (1734.4 ± 327.9 cells/mm^2) than that of the other candidate graft tendons, especially the quadriceps tendon (296.5 ± 49.2 cells/mm^2) (Table 3). Polarized light microscopy analysis of crimp morphology revealed interesting similarities and differences between the ACL and the knee tendons of interest (Figure 5). In all of the samples studied, crimp wavelengths appeared extremely uniform, with low amounts of intrafiber variation within the same specimen. The patellar tendon, quadriceps tendon, and semitendinosus tendon displayed longer crimp wavelengths compared with the ITB and ACL (Table 3). The mean crimp wavelength for the ACLs from 2 separate donors was 24.4 ± 3.2 μm.

Results for collagen fiber diameters were similar to those for crimp wavelengths, with the ITB being most similar to the ACL. Fibrils in the patellar tendon trended toward smaller diameters, while those in the semitendinosus tendon trended toward larger diameters. The fibrils in the quadriceps tendon were bimodally distributed between large and small diameters. The mean fibril

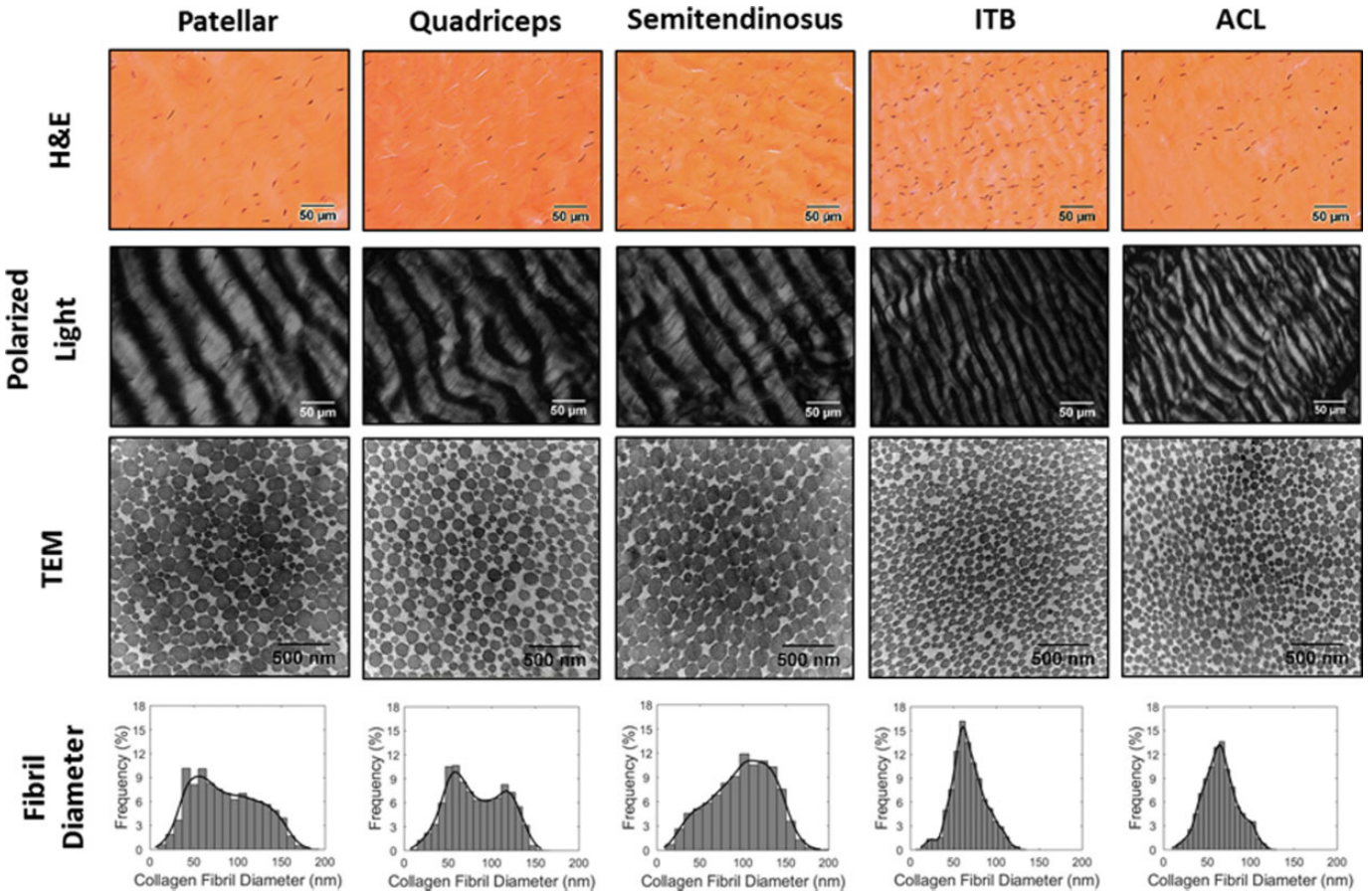

Figure 5. Histology, polarized light microscopy, and transmission electron microscopy (TEM) results for the pediatric patellar tendon, quadriceps tendon, semitendinosus tendon, iliotibial band (ITB), and anterior cruciate ligament (ACL) samples. First row: representative hematoxylin and eosin (H&E)–stained histology sections. Second row: representative polarized light microscopy images showing crimp morphology. Third row: TEM images showing collagen fibril cross sections. Fourth row: histograms of collagen fibril diameters.

TABLE 3
Microstructural Analysis Results for Pediatric ACLs and Candidate Graft Tendons[a]

	n	Fibroblast Density, cells/mm^2	Crimp Wavelength, µm	Collagen Fibril Diameter, nm
ACL	2-3[b]	829.6 ± 101.7	24.4 ± 3.2	65.3 ± 19.9
Patellar	1	606.1 ± 90.9	61.9 ± 8.7	86.4 ± 37.2
Quadriceps	1	296.5 ± 49.2	52.1 ± 5.6	82.6 ± 31.7
Semitendinosus	1	553.8 ± 115.5	48.5 ± 3.8	99.2 ± 35.6
ITB	1	1734.4 ± 327.9	27.0 ± 2.9	67.5 ± 19.5

[a]Data are shown as mean ± SD. ACL, anterior cruciate ligament; ITB, iliotibial band.
[b]Donor 4's fibroblast density and crimp wavelength were excluded.

diameter for the ACLs from 3 separate donors exhibited a distinctly unimodal distribution profile of 65.3 ± 19.9 nm (Appendix Figure A2).

DISCUSSION

Little is known about the mechanical behavior and microstructural properties of pediatric ACLs and the periarticular tissues most commonly utilized for their reconstruction. Results from this study demonstrated that mechanical properties were considerably weaker than what has been published in methodologically similar studies for the same structures in healthy adult populations (Figure 6). Interestingly, there are also relative differences in mechanical properties between the native ACL and autograft tendons in adults. For example, all 3 graft tissues have been shown to exhibit ultimate tensile loads and stiffnesses that are higher than those reported for the native ACL.[19,21,31,34,50,56] Adult hamstring tendons seem to possess the strongest mechanical properties and have previously been shown to exhibit significantly higher elastic modulus (1036 ± 312 MPa) and ultimate stress values (120.1 ± 30.0 MPa) than other graft candidates, including the patellar tendon (417 ± 107 MPa and 76.2 ± 25.1 MPa, respectively).[47] This is in agreement with our data for a pediatric population, which showed that

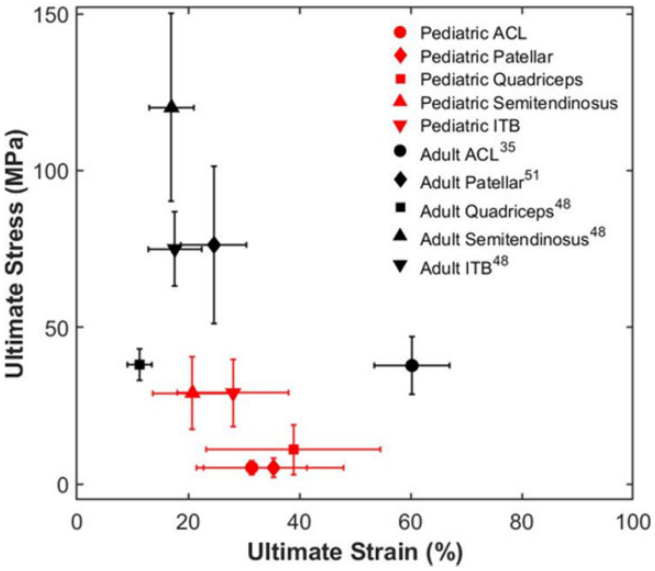

Figure 6. Ultimate stress-strain plot for the data presented by the current study (red points) compared with data reported in the adult population (black points). Data points represent the mean ultimate stress and ultimate strain, and error bars indicate the standard deviation. ACL, anterior cruciate ligament; ITB, iliotibial band.

the semitendinosus tendon and ITB were stronger and less compliant than the quadriceps or patellar tendons. We also found relatively large specimen-specimen variability in the mechanical data for our pediatric specimens, especially for the quadriceps tendon. This could be attributed to donor factors such as age, sex, body mass index, and physical activity level, which we could not control because of the rarity of the donor cohort. Large variations in the mechanical properties of adult tendons and ligaments have been previously reported in the literature[47] and have been further attributed to individual biological variation in collagen fiber maturity, fiber alignment, interfiber cross-linkage, and fiber-matrix interaction.[33]

Functional properties in tendons and ligaments have been shown to be influenced by the morphology of collagen fibrils. An examination of the microstructure in samples harvested from the same knee of 1 donor revealed distinct differences between the pediatric ACL and the 4 candidate graft tendons. Crimp morphology has been linked to tendon mechanical function, and there is evidence demonstrating that collagen crimp characteristics are strongly tendon type specific.[49] Collagen crimps function as a buffer to provide immediate longitudinal elongation in response to loads, and the nonlinear toe region of the stress-strain curve represents the extension of these crimps (see Figure 3B).[26] Past the transition point and into the linear region, the crimps are fully recruited, and resistance is provided by stretching of the collagen triple helix and the cross-linkages between these helices. In tendons and ligaments, a higher crimp frequency likely provides protection to the structure during sudden increases in intrinsic forces produced by muscular contractions and compressive joint loads.[12,45]

Results from the current study showed that the patellar, quadriceps, and semitendinosus tendons possessed a lower crimp frequency compared with the ITB and ACL. This may help to explain the slightly more prolonged toe region for the pediatric ACL (Table 2). The behavior of the toe region and transition point is often neglected in the literature, but it is important to document because ligament strains during activities of daily living and rehabilitation occur within this zone.[5,8] Beynnon and Fleming[5] demonstrated in an in vivo study that the strains in the midsubstance of the ACL rarely exceed 4% in both weightbearing and nonweightbearing activities involving varying degrees of knee extension. Using a mouse model, Miller et al[33] found that developmentally younger tendons required longer exposure to mechanical loading before structurally responding through uncrimping, resulting in higher transition strains. Interestingly, the pediatric ITB did not exhibit toe region properties similar to those of the ACL, which demonstrates that the uncrimping of collagen fibers is not the only mechanism driving toe region properties. For example, collagen fiber crimp frequency has been found to be dependent on the number of preconditioning cycles that are applied,[33] and it has also been suggested that crimp frequency is heterogeneous along the length of a tendon.[20,51]

The patellar, quadriceps, and semitendinosus tendons showed wider distributions of collagen fibril diameters than the ITB and ACL, which appeared to be predominantly composed of small-diameter fibrils (Figure 5). The mean fibril diameters for the patellar, quadriceps, and semitendinosus tendons were similar to the values reported in the literature for adult samples.[1,18,52] The mean fibril diameter for the pediatric ACL was considerably smaller than what has been reported for adults.[18] Little to no information exists in the literature regarding the collagen fibril ultrastructure for adult human ITBs. When considering animal models, Qu et al[42] found a significantly higher collagen fibril density and smaller fibril diameters in immature bovine ACLs (102 ± 11.6 nm) compared with a mature group (124.1 ± 22 nm). They also observed a unimodal distribution of fibril diameters in the immature group and a 3-fold increase in variance in the mature group. It is possible that the ACL and ITB are composed of immature networks of collagen fibers for a longer period of time than the semitendinosus, quadriceps, or patellar tendons.

The collagen fibril diameter size may be reflective of functional adaptations to physiological loads. Fibrils have been shown to be smaller and unimodally distributed at birth, becoming larger and bimodally distributed at maturity.[38,39] The existence of a true correlation between collagen fibril size and higher stiffness is controversial, but it is a likely contributor. Parry[37] posited that the bimodal distribution of fibril size was optimized so that larger fibrils provided high tensile strength and smaller fibers provided resistance to creep by increasing the density of interfibrillar electrostatic interactions.

This study has several limitations. Most notably, the sample size in this experiment was small. Because of the rarity of pediatric donors, this drawback is currently unavoidable. It was difficult to make direct comparisons between the current study and previous studies with adult cohorts. Differences in donor age, sex, physical condition, and skeletal maturity as well as graft size, ramp-to-failure

strain rate, graft construct configuration, method of CSA calculation, and clamping technique can all confound results.[8,56] The strength of tendons and ligaments has been shown to be dependent on the strain rate.[6,24] To minimize viscoelastic effects, the ramp-to-failure strain rate was kept at 0.03% per second, which was deliberately chosen to capture toe region properties. Previous studies have utilized strain rates as high as 100% per second to simulate the fast strain rate in accidents and acute injuries.[6,22,35] Bone insertions were not included in the grip-to-grip testing setup because the focus of this study was to characterize the intrinsic mechanical behavior of the tissues at the midsubstance. Although midsubstance failures have been reported, avulsions are more common within the pediatric population,[53] and an examination of the mechanical and microstructural properties at these regions is a logical next direction for further research. Many factors that are known to contribute to the ultimate failure load of an ACLR graft in vivo, such as graft size or graft folding and anchoring techniques, were not considered. Additionally, the anatomic direction of tension is not always axial. The ACL is structurally designed to withstand multiaxial stresses that can vary in direction and magnitude along the length of the tissue, which may lead to changes in mechanical and microstructural properties. Many studies have looked at the regional variation in tendon and ligament properties in adults, and the consideration of local strain measurements may be a direction for future research in the pediatric population.[2,4] Last, the specimens from this study were from donors aged 7 to 11 years. It is unclear whether the results from this study would be applicable to younger or older age groups without further research.

Clinical Implications

The surgical management of ACL deficiency in pediatric patients is complex, and many factors can contribute to graft selection for reconstruction. Optimizing ACLR in the pediatric patient population requires a more thorough understanding of anatomic graft placement, the mechanical properties of candidate grafts, the mechanical behavior and strength of anchoring techniques, and the biological processes that occur during graft incorporation. While the mechanical properties of the pediatric patellar tendon were almost identical to those of the pediatric ACL, the semitendinosus tendon and ITB were considerably stronger. As a result, these grafts may be able to resist the loads that make the ACL prone to reinjuries or that caused the injury in the first place. However, it is important to note that the ultimate failure load is dependent on the total CSA of the graft, which can fluctuate based on individual biological variation, graft harvest site, and whether multibundle reconstruction is performed.

Another important consideration is that the mechanical properties of ACLR grafts have been demonstrated to decrease during the postoperative ligamentization process and never return to normal.[43] These changes also appear to be accompanied by a shift in collagen fibril diameters from a bimodal to unimodal distribution over time.[1] It is possible that stronger graft candidates could undergo such reductions in mechanical properties and remain sufficient surrogates for the native ACL. Conversely, another concern with ACLR grafts is joint overconstraint with a surrogate tissue that is too stiff, which could potentially lead to increased joint contact pressures, an increased risk of osteoarthritis, and even an increased risk of early graft failure.[47] While some research has been conducted to examine the effects of graft tensioning and multibundle reconstruction on knee joint constraint, evidence of this occurring in the nonfolded candidate grafts examined in this study is scarce.[16,32]

CONCLUSION

The incidence of pediatric ACL injuries has increased significantly over the past several decades, as youth participation and specialization in sports have increased. Despite this, there is a dearth of information in the literature on the mechanical and microstructural properties of pediatric knee tendons and ligaments. Further optimization of the pediatric ACLR procedure such that the surrogate graft is the most appropriate mechanical and biological option for the patient will ultimately improve surgical outcomes. This study utilized a small and extremely rare sample of pediatric cadaveric knees to develop a comprehensive suite of data on the pediatric ACL and the most common tendons used for reconstruction in the pediatric knee. Our data showed that different autografts possess distinct mechanical properties that often differ markedly from the ACL. These data can be used to inform the selection of grafts for reconstruction and the design and fabrication of synthetic constructs and also to develop constitutive musculoskeletal models that can be applied to clinically relevant loading conditions that are difficult to test with bench-top experiments alone.

REFERENCES

1. Abe S, Kurosaka M, Iguchi T, Yoshiya S, Hirohata K. Light and electron microscopic study of remodeling and maturation process in autogenous graft for anterior cruciate ligament reconstruction. *Arthroscopy*. 1993;9(4):394-405.
2. Abramowitch SD, Zhang X, Curran M, Kilger R. A comparison of the quasi-static mechanical and nonlinear viscoelastic properties of the human semitendinosus and gracilis tendons. *Clin Biomech (Bristol, Avon)*. 2010;25(4):325-331.
3. Arbes S, Resinger C, Vécsei V, Nau T. The functional outcome of total tears of the anterior cruciate ligament (ACL) in the skeletally immature patient. *Int Orthop*. 2007;31(4):471-475.
4. Beaulieu ML, Carey GE, Schlecht SH, Wojtys EM, Ashton-Miller JA. On the heterogeneity of the femoral enthesis of the human ACL: microscopic anatomy and clinical implications. *J Exp Orthop*. 2016;3(1):14.
5. Beynnon BD, Fleming BC. Anterior cruciate ligament strain in-vivo: a review of previous work. *J Biomech*. 1998;31(6):519-525.
6. Blevins FT, Hecker AT, Bigler GT, Boland AL, Hayes WC. The effects of donor age and strain rate on the biomechanical properties of bone-patellar tendon-bone allografts. *Am J Sports Med*. 1994;22(3):328-333.
7. Blickenstaff KR, Grana WA, Egle D. Analysis of a semitendinosus autograft in a rabbit model. *Am J Sports Med*. 1997;25(4):554-559.
8. Chandrashekar N, Hashemi J, Slauterbeck J, Beynnon BD. Low-load behaviour of the patellar tendon graft and its relevance to the

biomechanics of the reconstructed knee. *Clin Biomech (Bristol, Avon)*. 2008;23(7):918-925.
9. Courvoisier A, Grimaldi M, Plaweski S. Good surgical outcome of transphyseal ACL reconstruction in skeletally immature patients using four-strand hamstring graft. *Knee Surg Sports Traumatol Arthrosc*. 2011;19(4):588-591.
10. Danto MI, Woo SL-Y. The mechanical properties of skeletally mature rabbit anterior cruciate ligament and patellar tendon over a range of strain rates. *J Orthop Res*. 1993;11(1):58-67.
11. DeLee J, Curtis R. Anterior cruciate ligament insufficiency in children. *Clin Orthop Relat Res*. 1983;172:112-118.
12. Diamant J, Keller A, Baer E, Litt M, Arridge RGC. Collagen: ultrastructure and its relation to mechanical properties as a function of ageing. *Proc R Soc Lond B Biol Sci*. 1972;180(1060):293-315.
13. Dodwell ER, LaMont LE, Green DW, Pan TJ, Marx RG, Lyman S. 20 years of pediatric anterior cruciate ligament reconstruction in New York State. *Am J Sports Med*. 2014;42(3):675-680.
14. Ellis HB, Matheny LM, Briggs KK, Pennock AT, Steadman JR. Outcomes and revision rate after bone–patellar tendon–bone allograft versus autograft anterior cruciate ligament reconstruction in patients aged 18 years or younger with closed physes. *Arthroscopy*. 2012; 28(12):1819-1825.
15. Frank JS, Gambacorta PL. Anterior cruciate ligament injuries in the skeletally immature athlete: diagnosis and management. *J Am Acad Orthop Surg*. 2013;21(2):78-87.
16. Friederich NF, O'Brien WR. Anterior cruciate ligament graft tensioning versus knee stability. *Knee Surg Sports Traumatol Arthrosc*. 1998; 6(1):S38-S42.
17. Gottschalk AW, Andrish JT. Epidemiology of sports injury in pediatric athletes. *Sports Med Arthrosc Rev*. 2011;19(1):2-6.
18. Hadjicostas PT, Soucacos PN, Koleganova N, Krohmer G, Berger I. Comparative and morphological analysis of commonly used autografts for anterior cruciate ligament reconstruction with the native ACL: an electron, microscopic and morphologic study. *Knee Surg Sports Traumatol Arthrosc*. 2008;16(12):1099-1107.
19. Hamner DL, Brown CH Jr, Steiner ME, Hecker AT, Hayes WC. Hamstring tendon grafts for reconstruction of the anterior cruciate ligament: biomechanical evaluation of the use of multiple strands and tensioning techniques. *J Bone Joint Surg Am*. 1999;81(4):549-557.
20. Hansen KA, Weiss JA, Barton JK. Recruitment of tendon crimp with applied tensile strain. *J Biomech Eng*. 2002;124(1):72-77.
21. Harris NL, Smith DA, Lamoreaux L, Purnell M. Central quadriceps tendon for anterior cruciate ligament reconstruction, part I: morphometric and biomechanical evaluation. *Am J Sports Med*. 1997;25(1):23-28.
22. Hashemi J, Chandrashekar N, Mansouri H, Slauterbeck JR, Hardy DM. The human anterior cruciate ligament: sex differences in ultrastructure and correlation with biomechanical properties. *J Orthop Res*. 2008;26(7):945-950.
23. Johnson GA, Tramaglini DM, Levine RE, Ohno K, Choi NY, Woo SL. Tensile and viscoelastic properties of human patellar tendon. *J Orthop Res*. 1994;12(6):796-803.
24. Kahn CJ, Wang X, Rahouadj R. Nonlinear model for viscoelastic behavior of Achilles tendon. *J Biomech Eng*. 2010;132(11):111002.
25. Kane PW, Wascher J, Dodson CC, Hammoud S, Cohen SB, Ciccotti MG. Anterior cruciate ligament reconstruction with bone-patellar tendon-bone autograft versus allograft in skeletally mature patients aged 25 years or younger. *Knee Surg Sports Traumatol Arthrosc*. 2016;24(11):3627-3633.
26. Kastelic J, Palley I, Baer E. A structural mechanical model for tendon crimping. *J Biomech*. 1980;13(10):887-893.
27. Kocher MS, Shore B, Nasreddine AY, Heyworth BE. Treatment of posterior cruciate ligament injuries in pediatric and adolescent patients. *J Pediatr Orthop*. 2012;32(6):553-560.
28. Kumar S, Ahearne D, Hunt DM. Transphyseal anterior cruciate ligament reconstruction in the skeletally immature: follow-up to a minimum of sixteen years of age. *J Bone Joint Surg Am*. 2013;95(1):e1.
29. Lake SP, Miller KS, Elliott DM, Soslowsky LJ. Effect of fiber distribution and realignment on the nonlinear and inhomogeneous mechanical properties of human supraspinatus tendon under longitudinal tensile loading. *J Orthop Res*. 2009;27(12):1596-1602.
30. Lake SP, Miller KS, Elliott DM, Soslowsky LJ. Tensile properties and fiber alignment of human supraspinatus tendon in the transverse direction demonstrate inhomogeneity, nonlinearity and regional isotropy. *J Biomech*. 2010;43(4):727-732.
31. Markolf KL, Burchfield DM, Shapiro MM, Davis BR, Finerman GA, Slauterbeck JL. Biomechanical consequences of replacement of the anterior cruciate ligament with a patellar ligament allograft, part I: insertion of the graft and anterior-posterior testing. *J Bone Joint Surg Am*. 1996;78(11):1720-1727.
32. Melby A, Noble JS, Askew MJ, Boom AA, Hurst FW. The effects of graft tensioning on the laxity and kinematics of the anterior cruciate ligament reconstructed knee. *Arthroscopy*. 1991;7(3):257-266.
33. Miller KS, Connizzo BK, Feeney E, Tucker JJ, Soslowsky LJ. Examining differences in local collagen fiber crimp frequency throughout mechanical testing in a developmental mouse supraspinatus tendon model. *J Biomech Eng*. 2012;134(4):041004.
34. Noyes FR, Butler DL, Grood ES, Zernicke RF, Hefzy MS. Biomechanical analysis of human ligament grafts used in knee-ligament repairs and reconstructions. *J Bone Joint Surg Am*. 1984;66(3):344-352.
35. Noyes FR, Grood ES. The strength of the anterior cruciate ligament in humans and Rhesus monkeys. *J Bone Joint Surg Am*. 1976;58(8): 1074-1082.
36. O'Brien TD, Reeves ND, Baltzopoulos V, Jones DA, Maganaris CN. Mechanical properties of the patellar tendon in adults and children. *J Biomech*. 2010;43(6):1190-1195.
37. Parry DA. The molecular fibrillar structure of collagen and its relationship to the mechanical properties of connective tissue. *Biophys Chem*. 1988;29(1):195-209.
38. Parry DA, Barnes GR, Craig AS. A comparison of the size distribution of collagen fibrils in connective tissues as a function of age and a possible relation between fibril size distribution and mechanical properties. *Proc R Soc Lond B*. 1978;203(1152):305-321.
39. Parry DA, Craig AS. Quantitative electron microscope observations of the collagen fibrils in rat-tail tendon. *Biopolymers*. 1977;16(5): 1015-1031.
40. Petrigliano FA, McAllister DR, Wu BM. Tissue engineering for anterior cruciate ligament reconstruction: a review of current strategies. *Arthroscopy*. 2006;22(4):441-461.
41. Pierce TP, Issa K, Festa A, Scillia AJ, McInerney VK. Pediatric anterior cruciate ligament reconstruction: a systematic review of transphyseal versus physeal-sparing techniques. *Am J Sports Med*. 2017;45(2): 488-494.
42. Qu D, Chuang PJ, Prateepchinda S, et al. Micro- and ultrastructural characterization of age-related changes at the anterior cruciate ligament-to-bone insertion. *ACS Biomater Sci Eng*. 2017;3(11): 2806-2814.
43. Scheffler SU, Unterhauser FN, Weiler A. Graft remodeling and ligamentization after cruciate ligament reconstruction. *Knee Surg Sports Traumatol Arthrosc*. 2008;16(9):834-842.
44. Schindelin J, Arganda-Carreras I, Frise E, et al. Fiji: an open source platform for biological image analysis. *Nat Methods*. 2012;9(7):676-682.
45. Screen HR, Lee DA, Bader DL, Shelton JC. An investigation into the effects of the hierarchical structure of tendon fascicles on micromechanical properties. *Proc Inst Mech Eng H*. 2004;218(2):109-119.
46. Shea KG, Pfeiffer R, Wang JH, Curtin M, Apel PJ. Anterior cruciate ligament injury in pediatric and adolescent soccer players: an analysis of insurance data. *J Pediatr Orthop*. 2004;24(6):623.
47. Smeets K, Bellemans J, Scheys L, Eijnde BO, Slane J, Claes S. Mechanical analysis of extra-articular knee ligaments, part two: tendon grafts used for knee ligament reconstruction. *Knee*. 2017;24(5):957-964.
48. Smeets K, Slane J, Scheys L, Claes S, Bellemans J. Mechanical analysis of extra-articular knee ligaments, part one: native knee ligaments. *Knee*. 2017;24(5):949-956.
49. Spiesz EM, Thorpe CT, Thurner PJ, Screen HRC. Structure and collagen crimp patterns of functionally distinct equine tendons, revealed by quantitative polarised light microscopy (qPLM). *Acta Biomater*. 2018;70:281-292.

50. Stäubli HU, Schatzmann L, Brunner P, Rincón L, Nolte L-P. Mechanical tensile properties of the quadriceps tendon and patellar ligament in young adults. *Am J Sports Med*. 1999;27(1):27-34.
51. Stouffer DC, Butler DL, Hosny D. The relationship between crimp pattern and mechanical response of human patellar tendon-bone units. *J Biomech Eng*. 1985;107(2):158-165.
52. Strocchi R, de Pasquale V, Gubellini P, et al. The human anterior cruciate ligament: histological and ultrastructural observations. *J Anat*. 1992;180(pt 3):515-519.
53. Toy JO, Feeley BT, Gulotta LV, Warren RF. Arthroscopic avulsion repair of a pediatric ACL with an anomalous primary insertion into the lateral meniscus. *HSS J*. 2011;7(2):190-193.
54. Vaughn NH, Jackson T, Hennrikus WL. Anterior cruciate ligament reconstruction using quadriceps tendon autograft in adolescent athletes [abstract]. *Pediatrics*. 2018;141:194.
55. Wan C, Hao Z, Wen S, Leng H. A quantitative study of the relationship between the distribution of different types of collagen and the mechanical behavior of rabbit medial collateral ligaments. *PLoS One*. 2014;9(7):e103363.
56. West RV, Harner CD. Graft selection in anterior cruciate ligament reconstruction. *J Am Acad Orthop Surg*. 2005;13(3):197-207.
57. Willimon SC, Jones CR, Herzog MM, May KH, Leake MJ, Busch MT. Micheli anterior cruciate ligament reconstruction in skeletally immature youths: a retrospective case series with a mean 3-year follow-up. *Am J Sports Med*. 2015;43(12):2974-2981.
58. Woo SL-Y, Hollis JM, Adams DJ, Lyon RM, Takai S. Tensile properties of the human femur-anterior cruciate ligament-tibia complex: the effects of specimen age and orientation. *Am J Sports Med*. 1991; 19(3):217-225.
59. Woo SL-Y, Newton PO, MacKenna DA, Lyon RM. A comparative evaluation of the mechanical properties of the rabbit medial collateral and anterior cruciate ligaments. *J Biomech*. 1992;25(4):377-386.
60. Zhao L, Thambyah A, Broom N. Crimp morphology in the ovine anterior cruciate ligament. *J Anat*. 2015;226(3):278-288.

APPENDIX

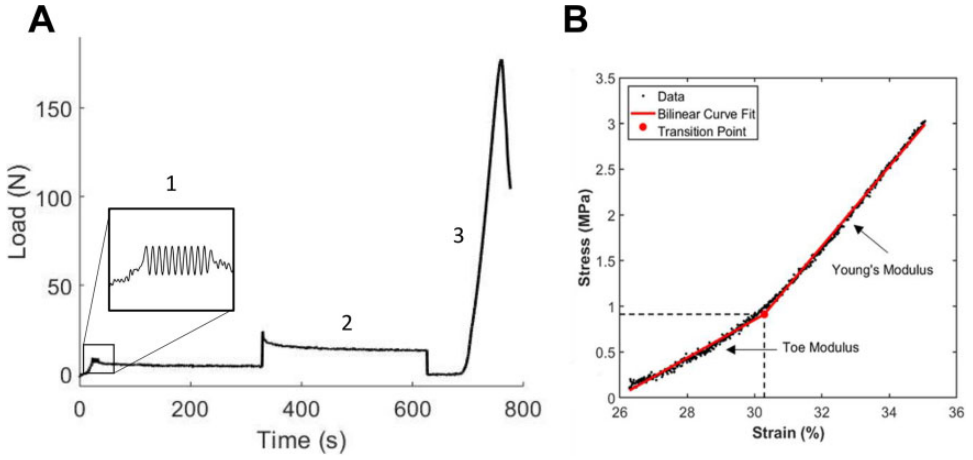

Figure A1. Schematic of the mechanical testing protocol. (A) Specimens were subjected to (1) preconditioning, (2) stress-relaxation, and (3) ramp-to-failure phases. (B) The stress-strain data from ramp to failure can be fit using a bilinear constitutive model to approximate the moduli in the toe and linear regions as well as the transition point.

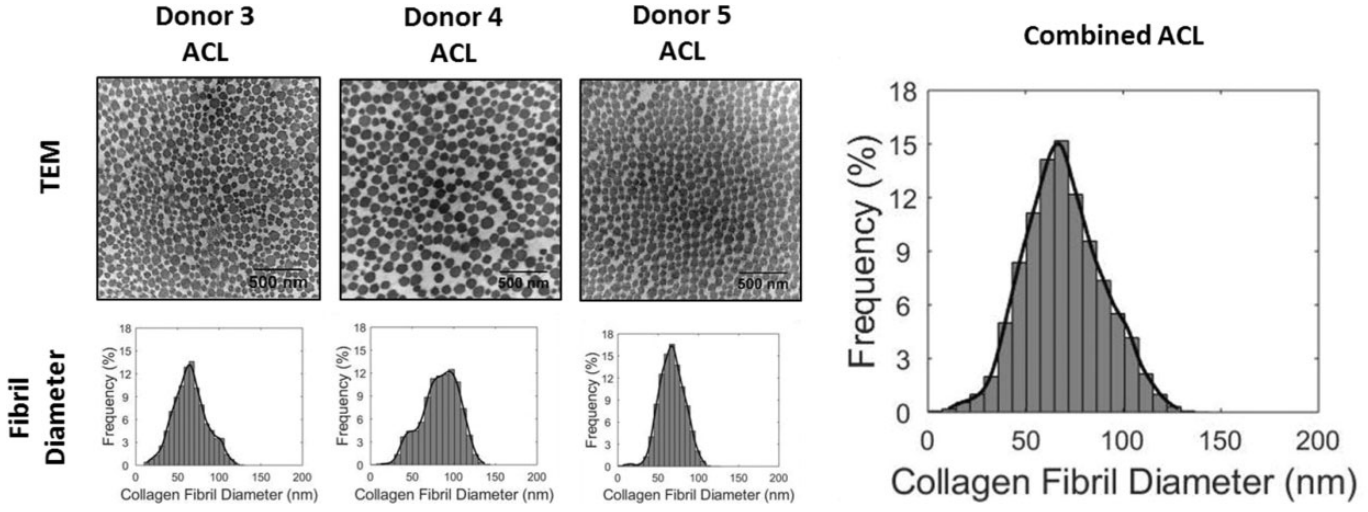

Figure A2. (Left) Representative transmission electron microscopy images of collagen fibril cross sections and histograms of collagen fibril diameters for 3 anterior cruciate ligament (ACL) samples from separate donors. (Right) Histogram of collagen fibril diameters pooled from data from all 3 ACLs.

TABLE A1
Results for Pediatric ACLs and Candidate Graft Tendons From Individual Donors[a]

	CSA, mm^2	Stress Relaxation, %	Ultimate Stress, MPa	Ultimate Strain, %	Young Modulus, MPa	Stiffness, N/mm	Strain Energy Density, MPa
ACL							
Donor 2	23.7	21.0	7.8	23.4	44.4	58.8	1.0
Donor 3	10.4	33.9	4.6	22.3	23.0	16.9	0.5
Donor 4	32.3	16.5	6.0	39.2	19.9	36.9	1.4
Donor 5	40.5	34.7	2.6	40.8	7.2	46.0	0.5
Patellar							
Donor 1	7.9	44.8	2.8	40.5	24.1	20.0	0.8
Donor 2	10.4	34.6	6.5	28.8	38.1	26.0	1.1
Donor 3	16.8	39.9	9.9	50.5	20.5	16.4	2.6
Donor 4	9.7	37.5	4.3	39.3	33.6	14.5	1.1
Donor 5	8.2	46.1	2.6	17.6	17.4	10.5	0.2
Quadriceps							
Donor 1	10.8	40.9	6.3	26.7	31.0	26.5	0.9
Donor 2	9.4	35.6	9.3	53.2	28.5	25.6	3.0
Donor 3	6.5	29.1	21.4	45.3	63.3	31.1	5.6
Donor 4	15.1	42.2	3.2	51.4	13.4	20.0	1.1
Donor 5	8.5	18.3	20.3	18.1	173.5	95.9	2.2
Semitendinosus							
Donor 1	8.7	33.2	39.8	26.7	231.0	112.1	4.1
Donor 2	10.7	29.6	14.5	11.2	212.1	122.2	0.8
Donor 3	9.4	25.7	20.6	15.0	211.9	99.7	1.4
Donor 4	9.4	21.2	29.0	24.6	141.7	76.3	3.5
Donor 5	8.8	24.0	41.1	26.4	189.3	93.7	5.3
ITB							
Donor 1	5.3	25.4	37.2	17.1	296.2	95.9	3.2
Donor 2	7.8	21.1	26.2	25.5	112.0	52.4	3.1
Donor 3	5.3	24.8	42.3	28.2	238.0	72.5	6.2
Donor 4	9.2	23.8	16.1	44.3	61.2	42.9	3.7
Donor 5	7.1	18.1	23.4	25.3	100.8	44.1	2.9

[a]ACL, anterior cruciate ligament; CSA, cross-sectional area; ITB, iliotibial band.

TABLE A2
Toe Region Results for Pediatric ACLs and Candidate Graft Tendons From Individual Donors[a]

	Transition Stress, MPa	Transition Strain, %	Toe Modulus, MPa
ACL			
Donor 2	0.9	4.0	20.7
Donor 3	0.8	4.1	15.1
Donor 4	1.0	5.6	13.3
Donor 5	0.3	8.1	3.4
Patellar			
Donor 1	0.4	3.0	13.3
Donor 2	0.6	2.4	26.6
Donor 3	0.3	2.5	11.5
Donor 4	0.6	3.0	18.5
Donor 5	0.2	2.3	14.8
Quadriceps			
Donor 1	0.4	3.0	15.5
Donor 2	0.4	2.4	15.8
Donor 3	1.1	3.1	27.4
Donor 4	0.3	2.7	9.2
Donor 5	2.9	2.8	100.0
Semitendinosus			
Donor 1	5.7	9.8	67.5
Donor 2	1.6	2.9	69.1
Donor 3	2.1	4.3	51.5
Donor 4	2.5	4.6	53.3
Donor 5	3.1	4.0	84.6
ITB			
Donor 1	2.7	2.7	108.3
Donor 2	2.1	4.4	48.9
Donor 3	2.4	4.9	54.8
Donor 4	4.4	15.4	29.1
Donor 5	2.4	3.8	53.6

[a]ACL, anterior cruciate ligament; ITB, iliotibial band.